JCTC Journal of Chemical Theory and Computation

Article

pubs.acs.org/JCTC

Stable and Efficient Linear Scaling First-Principles Molecular Dynamics for 10000+ Atoms

Michiaki Arita,[†,‡] David R. Bowler,[§,∥,⊥] and Tsuyoshi Miyazaki*[,‡,†]

[†]Faculty of Science and Technology, Tokyo University of Science, 2641 Yamasaki, Noda, Chiba 278-8510, Japan

[‡]Computational Materials Science Unit (CMSU), National Institute for Materials Science (NIMS), 1-1 Namiki, Tsukuba, Ibaraki 305-0044, Japan

[§]Department of Physics and Astronomy, University College London (UCL), Gower Street, London WC1E 6BT, U.K.

[∥]London Centre for Nanotechnology (LCN), University College London (UCL), 17-19 Gordon Street, London WC1H 0AH, U.K.

[⊥]International Center for Materials Nanoarchitectonics (MANA), National Institute for Materials Science (NIMS), 1-1 Namiki, Tsukuba, Ibaraki 305-0044, Japan

Supporting Information

ABSTRACT: The recent progress of linear-scaling or O(N) methods in density functional theory (DFT) is remarkable. Given this, we might expect that first-principles molecular dynamics (FPMD) simulations based on DFT could treat more realistic and complex systems using the O(N) technique. However, very few examples of O(N) FPMD simulations exist to date, and information on the accuracy and reliability of the simulations is very limited. In this paper, we show that efficient and robust O(N) FPMD simulations are now possible by the combination of the extended Lagrangian Born−Oppenheimer molecular dynamics method, which was recently proposed by Niklasson (*Phys. Rev. Lett.* **2008**, *100*, 123004), and the density matrix method as an O(N) technique. Using our linear-scaling DFT code CONQUEST, we investigate the reliable calculation conditions for accurate O(N) FPMD and demonstrate that we are now able to do practical, reliable self-consistent FPMD simulations of a very large system containing 32768 atoms.

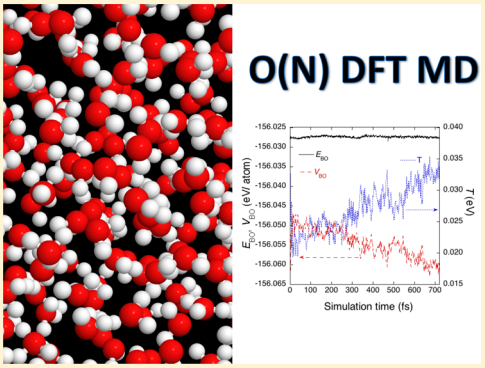

1. INTRODUCTION

First-principles molecular dynamics (FPMD) based on density functional theory (DFT) is a well-established and highly successful tool for studying reactions or processes of materials at the atomic scale. As a result of increases in computer power, the variety and complexity of the materials and phenomena investigated by FPMD simulations have been growing. However, the size of the systems modeled with FPMD simulations have remained limited to systems of a few hundred atoms in most cases because the computational cost of standard DFT methods grows rapidly, proportional to the cube of the number of atoms in the system (N). There are many demands to enlarge the system size in diverse fields, including computational physics, chemistry, materials science, biology, and so on. Examples of these problems include chemical reactions at liquid−solid interfaces, various processes in complex biological systems, and the growth mechanism of nanostructured materials at the atomic scale; in all of these cases, we have to treat systems containing many thousands or tens of thousands of atoms. In this respect, recent advances in developing linear-scaling or O(N) methods are encouraging.[1] There have been several demonstrations that efficient and reliable linear-scaling DFT calculations are now available to calculate the electronic structure, total energy, and atomic forces of very large systems, including up to millions of atoms.[2,3]

Although it is now possible to calculate the total energy and atomic forces of very large systems using O(N) DFT methods,[4−7] this does not guarantee that stable, efficient, and accurate FPMD simulations are possible in practice.[8] With conventional DFT methods, there are two widely used methods to achieve efficient FPMD simulations. The first method is known as Car−Parrinello MD (CPMD),[9] where the propagations of electronic structure and the atomic positions are treated simultaneously by introducing a fictitious mass for the electronic degree of freedom. This method is efficient, but the accuracy of the CPMD simulations can depend on the choice of the fictitious mass. By contrast, Born−Oppenheimer MD (BOMD) deals with the electronic and nuclear problems separately. In this method, the electronic structure in the ground state is calculated at each set of atomic positions, usually by optimization of the Kohn−Sham orbitals using an iterative method.[10] The BOMD method thus needs more CPU time than CPMD for each MD step, but the method is robust and stable and allows us to adopt a longer time step. As a result,

Received: September 22, 2014
Published: November 10, 2014

the CPU time needed for a whole MD simulation is tractable because the number of force calculations is smaller (the cost of calculating the atomic forces is usually much higher than that of updating the Kohn−Sham orbitals). The main problem facing this method, however, is that both the stability and the reliability of the MD depend on the accuracy of the calculated forces. If the optimization of the Kohn−Sham orbitals or the convergence of the self-consistent field is not sufficiently accurate, the method suffers from a systematic energy drift in microcanonical MD simulations due to the violation of time-reversal symmetry. This can also result in poor reliability for canonical MD simulations. Recently this problem has been solved using the extended Lagrangian Born−Oppenheimer MD (XL-BOMD) method proposed by Niklasson and co-workers,[11−13] whose Lagrangian includes auxiliary electronic degrees of freedom as dynamical variables to recover time-reversal symmetry in BOMD simulations. They have shown that BOMD simulations with long-term conservation of total energy are possible.

It is reasonable to expect that this recent progress with the XL-BOMD method could be used with O(N) DFT techniques. However, since linear-scaling methods rely on the locality of the electronic structure and need to introduce approximations to utilize this locality, the accuracy of the O(N) method may change during the MD simulations, and it is not clear how accurate or stable MD can be with O(N) DFT methods. Although there have already been a few reports showing examples of O(N) FPMD[14−17] or O(N) self-consistent tight-binding[18] simulations, they use different linear-scaling techniques and the information about the accuracy, stability, and efficiency of the simulations is rather limited. In this paper, we report the stability and accuracy of XL-BOMD simulations employing a density matrix minimization (DMM) technique,[19,20] which is one of the most common O(N) DFT methods. The accuracy of the forces calculated by the DMM method is high because the method satisfies the variational principle.[5] To our knowledge, the combination of DMM and XL-BOMD methods has not been investigated to date. Since the original XL-BOMD methods assume the orthogonality of the basis functions, the formulation of the method for nonorthogonal basis functions is also presented. We show that the XL-BOMD method can be introduced into our linear-scaling DFT code Conquest,[21−23] and we report that robust, accurate, and efficient FPMD is possible with the DMM method. Reliable calculation conditions for accurate O(N) FPMD are also investigated. In the end, we demonstrate that it is now possible to do actual FPMD simulations of a 32768-atom system.

The rest of the paper is organized as follows. In the next section, we present the methods and algorithms used or introduced in this work. In section 3, we report the results of the test calculations, the investigation of reliable calculation conditions, and some examples of the FPMD simulations, including that of the 32768-atom system. Finally, concluding remarks are given in section 4.

2. METHODS AND ALGORITHMS

The implementation of molecular dynamics and all of the calculations were performed with Conquest, which is a linear-scaling pseudopotential DFT code.[21−23] In order to achieve linear scaling in both computational time and memory consumption, the code works with the density matrix ρ rather than the wave functions because of its spatial locality:

$$\rho(\mathbf{r}, \mathbf{r}') \to 0 \text{ as } |\mathbf{r} - \mathbf{r}'| \to \infty \tag{1}$$

Conquest assumes that the density matrix can be described in a separable form:

$$\rho(\mathbf{r}, \mathbf{r}') = \sum_{i\alpha,j\beta} \phi_{i\alpha}(\mathbf{r}) K_{i\alpha,j\beta} \phi_{j\beta}(\mathbf{r}') \tag{2}$$

where $\phi_{i\alpha}$ is a nonorthogonal localized orbital called a *support function*, which is nonzero only within a sphere centered at atom i, and α denotes the support functions of a given atom.

Support functions are represented in terms of localized basis functions; in Conquest we can use systematically improvable basis functions (B-splines[24]) or pseudoatomic orbitals (PAOs).[4,25] $K_{i\alpha,j\beta}$ is an element of the density matrix represented in terms of the support functions. We find the electronic ground state by minimizing the total energy with respect to the density matrix while imposing the correct electron number and weak idempotency. The complete minimization combines two algorithms:[26] McWeeny's iterative purification[27,28] and the auxiliary density matrix (ADM) method proposed by Li, Nunes, and Vanderbilt.[19] An initial density matrix is generated starting from the Hamiltonian (scaled to have the right trace and eigenvalue spectrum) using the extension of McWeeny's approach for the canonical case.[28]

In the ADM method, weak idempotency is imposed by expressing the density matrix $\mathbf{K}$ in terms of an auxiliary density matrix $\mathbf{L}$ and the support function overlap matrix $\mathbf{S}$ ($S_{i\alpha,j\beta} = \langle \phi_{i\alpha} | \phi_{j\beta} \rangle$) as follows:

$$\mathbf{K} = 3\mathbf{LSL} - 2\mathbf{LSLSL} \tag{3}$$

The spatial truncation of the density matrix is actually imposed on the $\mathbf{L}$ matrix, such that $L_{i\alpha,j\beta} = 0$ once $|\mathbf{R}_i - \mathbf{R}_j| \geq R_L$; this is called the "$\mathbf{L}$ range" in the rest of this report.

McWeeny's procedure is applied until the energy rises (a sign of reaching truncation error[28]). The $\mathbf{L}$ matrix is then passed into the ADM, which is a variational approach, using a modified Pulay/Broyden algorithm. This part of the minimization is called density matrix minimization (DMM).

In this paper, we represent each support function $\phi_{i,\alpha}(r)$ in terms of one PAO (the approach given here can easily be extended to the case where we also minimize the energy with respect to the PAOs, which will be presented in a future publication). In running BOMD simulations with the DMM method, we have two ways to optimize the electronic structure. One is to initialize the density matrix using McWeeny's procedure at every atom movement. The initial charge density is made from the superposition of the atomic charge densities. Since the Hamiltonian and overlap matrices are recalculated after the movement of atoms, the initial matrix $\mathbf{L}$ and the subsequent optimized $\mathbf{L}$ matrix will maintain time-reversal symmetry; we hence expect that BOMD simulations should conserve energy and be stable. The other method is to utilize the ADM found from the previous MD step to start the present DMM. In this case, the initial charge density is made from the initial density matrix $\mathbf{L}$ prepared for the present DMM and is updated with the $\mathbf{L}$ matrix simultaneously during the DMM. This method is more efficient but breaks the time-reversal symmetry, potentially leading to unphysical energy drift.

To maintain time-reversal symmetry while keeping the efficiency of density matrix reuse, we use the extended Lagrangian scheme proposed by Niklasson.[12] We introduce into the Born−Oppenheimer Lagrangian $\mathcal{L}^{\mathrm{XBO}}$ an auxiliary

degree of freedom **X** that is associated with **LS** rather than **L** to maintain the correct nonorthogonal metric:[29]

$$\mathcal{L}^{\mathrm{XBO}}(\mathbf{X}, \dot{\mathbf{X}}, \mathbf{R}, \dot{\mathbf{R}}) = \mathcal{L}^{\mathrm{BO}}(\mathbf{R}, \dot{\mathbf{R}}) + \frac{\mu}{2}\mathrm{Tr}[\dot{\mathbf{X}}^2] - \frac{\mu\omega^2}{2}\mathrm{Tr}[(\mathbf{LS} - \mathbf{X})^2] \quad (4)$$

X is a sparse matrix with the range of the matrix **LS**, μ the fictitious electronic mass, and ω is the curvature of the electronic harmonic potential. As in the original XL-BOMD method, if we take the limit $\mu \to 0$, $\mathcal{L}^{\mathrm{XBO}}$ becomes $\mathcal{L}^{\mathrm{BO}}$ and we have equations of motion for the nuclear positions and **X**. If we apply the time-reversible Verlet scheme to calculate **X** using the equation of motion, we have

$$\mathbf{X}(t + \delta t) = 2\mathbf{X}(t) - \mathbf{X}(t - \delta t) + \delta t^2\omega^2[\mathbf{L}(t)\mathbf{S}(t) - \mathbf{X}(t)] \quad (5)$$

which shows that $\mathbf{X}(t)$ is time-reversible and evolves in a harmonic potential centered around the ground-state $\mathbf{L}(t)\mathbf{S}(t)$. This also implies that a good initial guess for the **L** matrix, which will obey time-reversal symmetry, can be calculated by multiplying **X** and $\mathbf{S}^{-1}$ (in CONQUEST, the sparse approximate inverse **S** is computed using Hotelling's method[30]).

Even though the time-reversibility is maintained during propagation, the **X** matrix tends to move away from the harmonic center over time. As a result, the number of iterations to reach the ground state at each MD step gradually increases in the course of a simulation. To remove accumulated numerical errors, we add a dissipative force to the propagation of **X**, following ref 31:

$$\mathbf{X}(t + \delta t) = 2\mathbf{X}(t) - \mathbf{X}(t - \delta t) + \kappa[\mathbf{L}(t)\mathbf{S}(t) - \mathbf{X}(t)] + \alpha \sum_{m=0}^{M} c_m \mathbf{X}(t - m\delta t) \quad (6)$$

Here the parameters κ, α, and c_m are determined to ensure that the dissipation term does not significantly break the time-reversal symmetry; we used the values in ref 31. The amount of dissipation is controlled with a single parameter M, which determines the order of the polynomial, and we used $M = 5$ in the present work. With the dissipation term, we can keep the kinetic energy of $\dot{\mathbf{X}}$ small, thereby keeping $\mathbf{X}(t)$ close to the present ground-state $\mathbf{L}(t)\mathbf{S}(t)$. As a result, we would expect the number of DMM steps to be reduced. The effect of the dissipation term in the practical calculations is reported and discussed in section 3.1.

3. RESULTS

We will present our tests of the implementation of O(N) DFT in different stages: first, we will consider approaches that permit energy conservation and their efficiencies; second, we will discuss the effect of density matrix range and minimization tolerance; and finally, we will present practical calculations.

3.1. Effective Schemes for Linear-Scaling BOMD. First, we explore methods to achieve energy conservation with O(N) DFT and BOMD. We monitor the Born–Oppenheimer total energy (E_{BO}), which is defined as the sum of the ionic kinetic energy T and the DFT total energy V_{BO}. In the microcanonical ensemble, E_{BO} should be constant and thus is a good indicator to judge whether a simulation is accurately carried out. In what follows, R_{L} was set to 16 bohr (the effect of changing this value is explored below in section 3.2). Single-ζ (SZ) PAOs are used to represent support functions,[32] and the local density approximation (LDA) to the exchange–correlation functional with the parametrization by Perdew and Zunger[33] is adopted. MD simulations are conducted via the velocity-Verlet integrator[34] with a time step of 0.5 fs (fs) in a microcanonical ensemble; the initial velocities are given randomly to ensure that the Maxwell–Boltzmann distribution at 300 K holds. The same conditions are set in other simulations in this report, unless otherwise specified.

For a first run, we perform BOMD on 64-atom crystalline silicon with density matrix initialization by McWeeny steps, so the density matrix is initialized from the Hamiltonian at each MD step. The density matrix is updated until the residual in the DMM step, $(1/N)\ \mathrm{Tr}(\sigma\mathbf{S}^{-1}\sigma\mathbf{S}^{-1})$ with $\sigma = \delta E'/\delta\mathbf{L}$, becomes smaller than a given tolerance ϵ_{L}. Here, E' is defined as $V_{\mathrm{BO}} - \mu N_{\mathrm{el}}$, where N_{el} is the number of electrons and the Lagrange multiplier μ is used to keep the number of electrons fixed. The profile of the Born–Oppenheimer energy E_{BO} is shown by the solid line in Figure 1, and it is clear that the total energy is

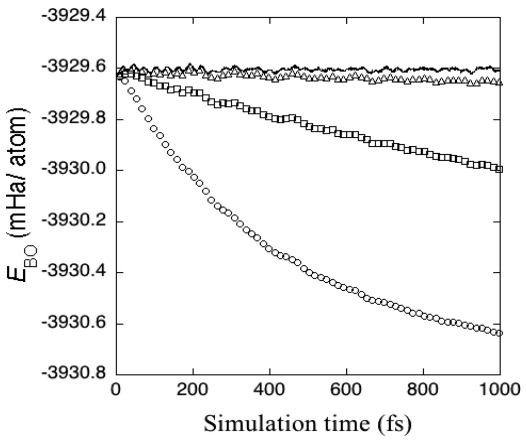

Figure 1. Born–Oppenheimer total energy (E_{BO}) profiles obtained by McWeeny initialization at every step (solid line) and by reusing the **L** matrix from the previous step for different tolerances ϵ_{L} (symbols). Symbols stand for $\epsilon_{\mathrm{L}} = 1.6 \times 10^{-5}$ (circles), 1.6×10^{-7} (squares), and 1.6×10^{-9} (triangles).

conserved even for a low DMM tolerance, $\epsilon_{\mathrm{L}} = 1.6 \times 10^{-5}$. However, this simulation is time-consuming since the electronic structure is calculated from scratch at every atom movement.

We now consider the reuse of the optimized **L** matrix from the previous MD step. When the optimized **L** matrix from the previous step is used to initialize the density matrix, the CPU time is significantly reduced. However, along with this improved efficiency we observe a significant and undesired energy drift, as shown in Figure 1 with symbols. Here we consider various values for the tolerance applied to the density matrix minimization, ϵ_{L}. The energy drift can be reduced by using a tighter ϵ_{L}, but tighter tolerance rapidly increases the number of DMM iterations and the computational cost.

In order to solve the problem of both accuracy and efficiency, we carry out XL-BOMD with $\epsilon_{\mathrm{L}} = 1.6 \times 10^{-5}$. Its E_{BO} profile (crosses in Figure 2) agrees extremely well with that of BOMD with density-matrix initialization by means of a McWeeny step (solid line in Figure 2), implying that XL-BOMD yields a well-conserved energy with lower computational requirements. However, there is a problem in efficiency with the method, as explained in section 2. After a long simulation time, the number of DMM iterations required to find the ground-state

dx.doi.org/10.1021/ct500847y | J. Chem. Theory Comput. 2014, 10, 5419–5425

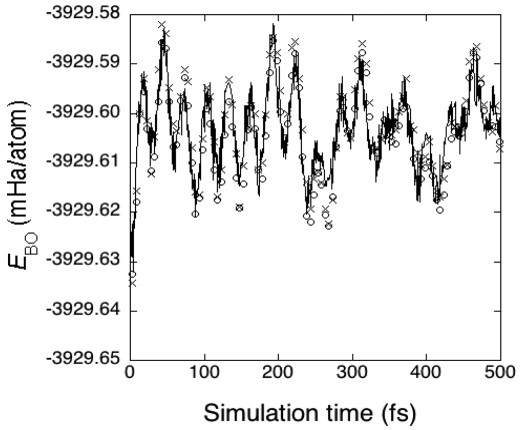

Figure 2. E_{BO} profiles with tolerance $\epsilon_L = 1.6 \times 10^{-5}$ and different initializations: McWeeny initialization at each MD step (solid line), XL-BOMD with dissipative force (circles), and XL-BOMD without dissipative force (crosses).

density matrix grows. This growing cost can be suppressed by applying a dissipative force, and the resulting E_{BO} profile (circles in Figure 2) is still very close to the profile without dissipation. A comparison of the required number of DMM iterations at each step for these different approaches is shown in Table 1. The reduction in computational cost obtained by using

Table 1. Numbers of DMM Iterations Required for Each MD Step for BOMD with Density Matrix Initialization by McWeeny Steps and XL-BOMD in the Presence (Y) or Absence (N) of a Dissipative Force[a]

type of run	dissipation	average	max	min
BOMD	N	10	12	8
XL-BOMD	N	6.7	8	2
XL-BOMD	Y	3.9	4	2

[a]The reported values are averages taken over 1000 steps.

XL-BOMD with dissipation is significant. Besides the smaller number of DMM iterations, the method does not require McWeeny steps, which typically include a few tens of matrix multiplications for purification (as in eq 3).

3.2. Effects of Density Matrix Range and Tolerance on XL-BOMD. In the last section, we showed that XL-BOMD simulations with the DMM method are robust and efficient using one typical set of calculation conditions. We now investigate how the MD results are affected by the parameters that control the accuracy and efficiency of linear-scaling DFT calculations with DMM. There are two key parameters: the range applied to the auxiliary density matrix (the **L** range or R_L) and the tolerance applied to the minimization (ϵ_L). In both tests, XL-BOMD is performed on 64-atom crystalline silicon with a dissipative force.

3.2.1. R_L Dependence. The key approximation made in linear scaling is to localize the density matrix, and it is vital to examine how the conservation of the energy E_{BO} is affected by the range, i.e., the parameter R_L. We test three values of R_L (13, 16, and 20 bohr), each with a strict DMM tolerance ($\epsilon_L = 1.6 \times 10^{-7}$). The simulations are performed for 2 ps (or 4000 steps).

The time-averaged BO total energies are very different for the three ranges (−106.830, −106.930, and −106.987 eV/atom for R_L = 13, 16, and 20 bohr, respectively) simply because the potential energy is lower for longer ranges. We plot the instantaneous energy fluctuations for the three ranges in Figure 3; the time-averaged absolute fluctuations, $\langle|\Delta E_{BO}|\rangle$, are 0.24,

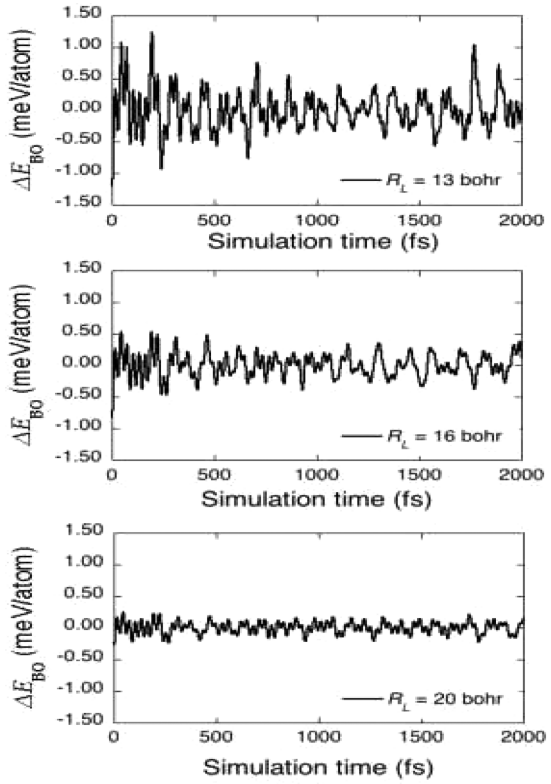

Figure 3. Instantaneous energy fluctuations calculated at three R_L values: 13 bohr (top), 16 bohr (middle), and 20 bohr (bottom).

0.15, and 0.075 meV/atom, respectively. These fluctuations become smaller as the range increases, and no energy drift is seen for any of the ranges.

During MD, atoms move into and out of the density matrix range, and we might expect to see energy drift and deviations at smaller ranges compared with longer ranges. The lack of drift is extremely encouraging, showing that the XL-BOMD approach is well-suited to both orthogonal and nonorthogonal basis sets and to linear-scaling approaches. It is also encouraging that, for relatively modest ranges, good accuracy is seen. We plot the kinetic energy of the ions in Figure 4. Although there is a deviation for the 13 bohr range after 2−300 fs, the 16 bohr range profile is extremely close to the 20 bohr range profile, and therefore, this range can be used with confidence over at least 1 ps.[35]

3.2.2. ϵ_L Dependence. The other main parameter that must be tested for its effect on the accuracy and stability of linear-scaling MD is the DMM tolerance ϵ_L. From the results of the last section, we fix the **L** range to 16 bohr and apply a wide range of ϵ_L from 10^{-4} to 10^{-7}; we assume that the results with $\epsilon_L = 10^{-7}$ can be regarded as reference values. We plot the BO total energy over a set of 1 ps simulations in Figure 5. First we note that E_{BO} with $\epsilon_L = 10^{-4}$ (circles) is not fully converged and is higher than the converged value by about 2 meV/atom. However, as we see in Figure 6, the kinetic energy profile shows almost perfect agreement with the reference profile with $\epsilon_L = 10^{-7}$, indicating that forces and hence the ionic kinetic energy converge faster than the total energy. It should be noted that we can achieve good convergence for both E_{BO} and T with ϵ_L =

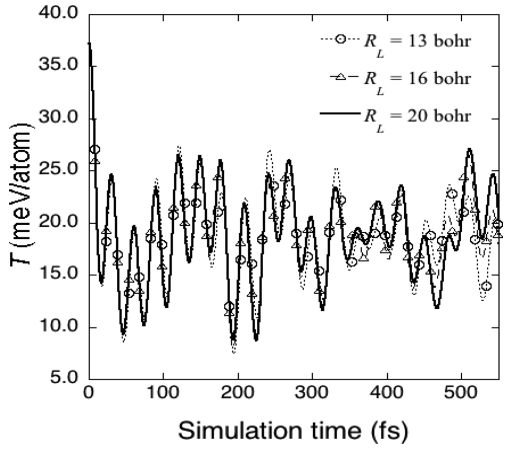

Figure 4. Ionic kinetic energy profiles for three R_L values: 13 bohr, 16 bohr, and 20 bohr.

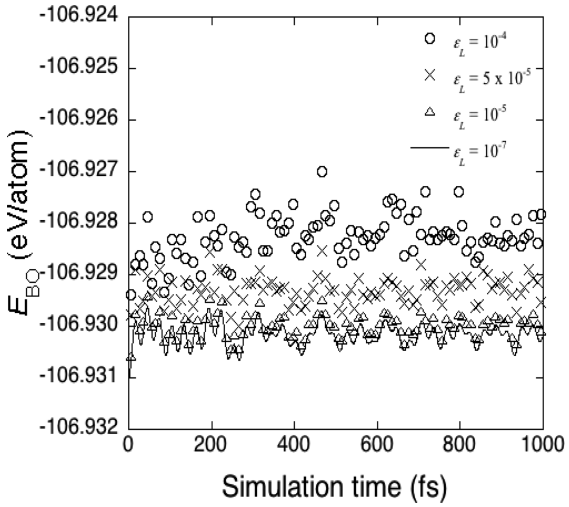

Figure 5. E_{BO} profiles calculated for different ϵ_L values. Circles, squares, and triangles denote the profiles calculated with $\epsilon_L = 10^{-4}$, 5×10^{-5}, and 10^{-5}, respectively. The solid line shows the profile calculated with $\epsilon_L = 10^{-7}$.

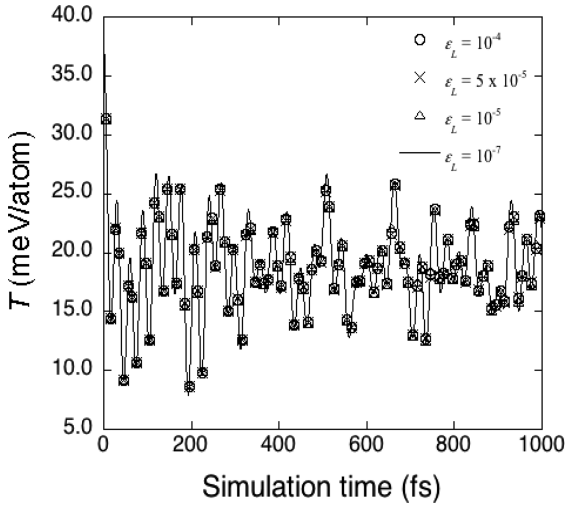

Figure 6. Ionic kinetic energy profiles calculated for different ϵ_L values. Circles, crosses, and triangles denote the profiles calculated with $\epsilon_L = 10^{-4}$, 5×10^{-5}, and 10^{-5}, respectively. The solid line shows the profile calculated with $\epsilon_L = 10^{-7}$.

10^{-5}. In addition, the E_{BO} profiles are close to each other for all tolerances except for a constant shift in the energy. Because of the fast convergence in ionic kinetic energy and the similarities in the E_{BO} profiles, the calculated trajectories will be very close. Hence, the DMM tolerance of 10^{-4} will give accurate simulations.

3.3. Practical O(*N*) MD Simulations. Having investigated the effects of the parameters on the simulations, we now present applications of the CONQUEST code to practical MD simulations using a double-ζ plus polarization (DZP) PAO basis, which is commonly used as a converged basis set. Three different systems are presented: eight-atom crystalline silicon, 32 water molecules, and a 32768-atom crystalline silicon cell to demonstrate the application to a large system. For all systems, the **L** range is set to 16 bohr. The initial temperature is 300 K and the time step of the simulation is 0.5 fs, unless stated otherwise.

3.3.1. Eight-Atom Bulk Silicon. Our first example is a small sample of crystalline silicon. We show E_{BO} calculated with $\epsilon_L = 1.3 \times 10^{-4}$ in Figure 7. This plot demonstrates excellent energy

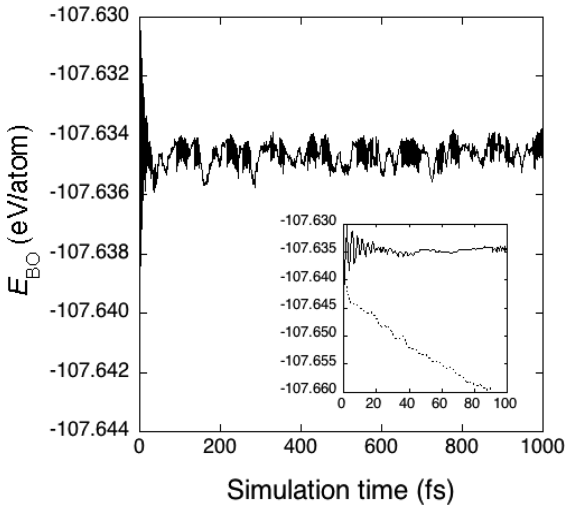

Figure 7. E_{BO} profile of crystalline Si with a DZP basis set. The inset shows a comparison of two approaches to XL-BOMD, with solid and dotted lines indicating the corrected and noncorrected propagators, respectively.

conservation, though there are large fluctuations for the first few femtoseconds. This initial large amplitude is probably caused by the system not being in an equilibrium state at the start of the simulation and is not a significant problem. In the inset of Figure 7, we also show the result of a simulation where we set **S** = **1** in eqs 4 and 5 (by supposing that **L** is expressed using orthogonal basis sets). By comparing the result (dotted line) with the correct one (solid line), we see that the former energy exhibits significant drift while the latter one is well-behaved. This indicates the importance of the metric used for nonorthogonal basis functions.

We perform another MD simulation on the same system using the same calculation conditions except that the time step is increased to 2.0 fs (the results are shown in the Supporting Information). We see that the large oscillations observed in the early stage are even larger and the time to suppress them becomes longer. However, it is found that the time evolution of the kinetic energy of Si atoms is almost the same in these two MD simulations. This result means that a time step of 2.0 fs can

dx.doi.org/10.1021/ct500847y | J. Chem. Theory Comput. 2014, 10, 5419−5425

be used to do reliable MD simulations on this silicon system. It is encouraging that we can use such a large time step for O(N) FPMD simulations. Here we should note that a new, efficient method that does not require self-consistent field optimization has been recently proposed[36] within the XL-BOMD framework. Introducing such new techniques to the CONQUEST code may even further accelerate the speed of O(N) FPMD simulations.

3.3.2. Box of 32 Water Molecules. We take a box of water made up of 32 molecules as our next target. Water is important as a system in its own right as well as forming the environment for most biological simulations. We perform linear-scaling XL-BOMD with ϵ_L set to 10^{-4} and using the GGA-PBE exchange-correlation functional,[37,38] as it describes water better than the LDA (we note that the convergence with respect to the grid may be slower for GGA). In Figure 8 we show the total energy

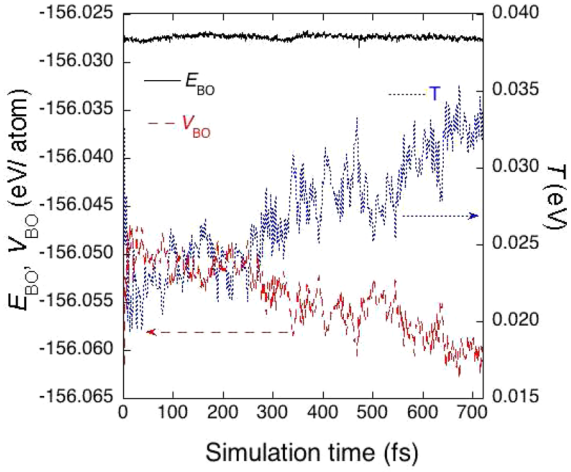

Figure 8. Born−Oppenheimer energy profiles of the water box system with DZP and PBE. The solid line represents E_{BO}, and the red dashed and blue dotted lines characterize its components V_{BO} and T, respectively.

E_{BO}, the ionic kinetic energy T, and the potential energy V_{BO}. We see that there are no initial large oscillations, unlike the silicon case, and that T appears to keep increasing during the run. This behavior is seen because we use the microcanonical ensemble and the simulation time is too short to reach a steady state. Even in such a situation showing fast changes, the averaged fluctuations are ∼1.1 meV/atom and good energy conservation is found without any energy drift. These results clearly demonstrate that there are no effects from the grid on the stability and accuracy of MD.

3.3.3. 32768-Atom Crystalline Silicon. Finally, as a demonstration of the scalability of our approach, we apply our algorithm to a large system: a 32768-atom crystalline silicon sample. The time evolution of the BO total energy and potential energy is shown in Figure 9. This is our first substantial attempt to examine the stability of an MD simulation on massive systems. This simulation is conducted under the same conditions as those in the eight-atom system in Figure 7, except that the time step is set to 2.0 fs.

We observe some similarities to the previous results. In the early stage of a simulation, large oscillations in the energy are seen, but they are gradually suppressed during the MD run. The time to suppress the large oscillations is longer than that in Figure 7 but similar to the case using 2.0 fs for eight-atom

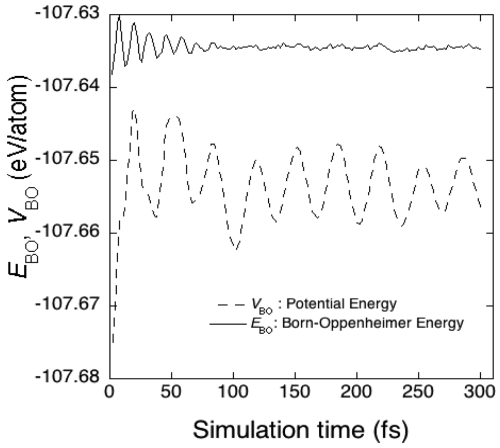

Figure 9. Profiles of the Born−Oppenheimer total energy and potential energy of a 32768-atom crystalline silicon system with the DZP basis set and LDA functional.

crystalline silicon (see Figure S1 in the Supporting Information). Thus, this comes from the difference in the time step and not from the system size. The energy fluctuations after 100 fs are smaller than 1 meV/atom and there is no energy drift, as shown in Figure 9. Although we carried out only a short MD run, the simulation is expected to remain stable in longer cases without any drift on the basis of the preceding example of an eight-atom system. Moreover, our approach is expected to ensure great stability on even larger and more complex systems by virtue of the high computational efficiency realized in the CONQUEST code.[2,3,39] The average time required for 1 MD step is 1085 s using 1024 CPUs (with 16 cores/CPU) of Fujitsu FX10. We are confident that this wall-clock time will be greatly reduced in the near future because the code is not optimized at present, especially for the part updating the **X** matrices; for simplicity, we now use a simple disk-based I/O procedure to read and write matrix elements of **X** matrices in the previous steps, and this part will be improved in the near future.

4. CONCLUSIONS

In this paper, we have investigated the efficiency, stability, and accuracy of MD simulations with the CONQUEST code using the DMM linear-scaling approach in order to demonstrate large-scale O(N) FPMD simulations in practice. We first found that accurate MD simulations can be performed by calculating the electronic structure from scratch using the McWeeny procedure at every atomic configuration. This gives excellent energy conservation even with a rather rough tolerance on the convergence of the density matrix minimization. However, this method requires considerable computational time because it initializes the density matrix at each step rather than reutilizing it.

Direct reuse of the optimized density matrix reduces the computational costs considerably but causes an unphysical energy drift. In order to achieve both accuracy and efficiency, we have introduced the XL-BOMD formalism proposed by Niklasson into the CONQUEST code, formulated for non-orthogonal basis functions. The application of XL-BOMD turns out to be much more efficient than the McWeeny approach, especially with the aid of a dissipative force, and good energy conservation is observed. We studied how the calculated results depend on two parameters specific to the DMM

dx.doi.org/10.1021/ct500847y | J. Chem. Theory Comput. 2014, 10, 5419−5425

method: the cutoff range of the **L** matrix and the tolerance applied to the density matrix minimization. We found that larger **L** ranges result in smaller energy fluctuations. Moreover, we found that the MD trajectories from runs with different ranges are almost identical, even when the Born−Oppenhimer total energy is not fully converged. This indicates that, as is well-known, the atomic forces converge much faster than the total energy with respect to these two parameters.

As practical applications, we treated crystalline silicon with LDA and liquid water with GGA. For the crystalline silicon, we demonstrated that accurate MD runs can be performed on very large systems, in this case containing 32768 atoms, but the method is scalable to significantly larger systems. The algorithms presented in this paper are applicable to a canonical ensemble and thus will open doors to more practical calculations on very large and complex systems.

■ ASSOCIATED CONTENT

Supporting Information

We present a comparison of the profiles of Born−Oppenheimer and kinetic energy using different time steps (0.5 and 2.0 fs) and show that the trajectories of the ions are almost the same. Results for crystalline silicon made of 4096 atoms using an initial temperature of 600 K are also provided, and we see that the energy convergence is excellent. This material is available free of charge via the Internet at http://pubs.acs.org.

■ AUTHOR INFORMATION

Corresponding Author

*E-mail: MIYAZAKI.Tsuyoshi@nims.go.jp.

Notes

The authors declare no competing financial interest.

■ ACKNOWLEDGMENTS

The authors thank Lianheng Tong and Takao Otsuka for fruitful discussions. This work was partly supported by KAKENHI projects by MEXT (22104005) and JSPS (26610120 and 26246021), Japan. Support from Strategic Programs for Innovative Research (SPIRE) and the Computational Materials Science Initiative (CMSI) is also acknowledged. Calculations were performed using the Numerical Materials Simulator at NIMS (Tsukuba, Japan), the K computer at RIKEN Advanced Institute for Computational Science (AICS) (Kobe, Japan), and the Fujitsu FX10 system at the Information Technology Center, University of Tokyo (Tokyo, Japan).

■ REFERENCES

(1) Bowler, D. R.; Miyazaki, T. *Rep. Prog. Phys.* **2012**, *75*, No. 036503.
(2) Bowler, D. R.; Miyazaki, T. *J. Phys.: Condens. Matter* **2010**, *22*, No. 074207.
(3) Arita, M.; Arapan, S.; Bowler, D. R.; Miyazaki, T. *J. Adv. Simulat. Sci. Eng.* **2014**, *1*, 87−97.
(4) Soler, J. M.; Artacho, E.; Gale, J. D.; García, A.; Junquera, J.; Ordejón, P.; Sánchez-Portal, D. *J. Phys.: Condens. Matter* **2002**, *14*, 2475−2779.
(5) Miyazaki, T.; Bowler, D. R.; Choudhury, R.; Gillan, M. J. *J. Chem. Phys.* **2004**, *121*, 6186−6194.
(6) Hine, N. D. M.; Robinson, M.; Haynes, P. D.; Skylaris, C.-K.; Payne, M. C.; Mostofi, A. A. *Phys. Rev. B* **2011**, *83*, No. 195102.
(7) Osei-Kuffuor, D.; Fattebert, J.-L. *Phys. Rev. Lett.* **2014**, *112*, No. 046401.
(8) Bowler, D.; Miyazaki, T.; Truflandier, L. A.; Gillan, M. J. *Comment on "Accurate and Scalable O(N) Algorithm for First-Principles Molecular-Dynamics Computations on Large Parallel Computers.* 2014, arXiv:1402.6828. arXiv.org eprint archive. http://arxiv.org/abs/1402.6828 (accessed Sept 22, 2014).
(9) Car, R.; Parrinello, M. *Phys. Rev. Lett.* **1985**, *55*, 2471−2474.
(10) Payne, M. C.; Teter, M. P.; Allan, D. C.; Arias, T. A.; Joannopoulos, J. D. *Rev. Mod. Phys.* **1992**, *64*, 1045−1097.
(11) Niklasson, A. M. N.; Tymczak, C. J.; Challacombe, M. *Phys. Rev. Lett.* **2006**, *97*, No. 123001.
(12) Niklasson, A. M. N. *Phys. Rev. Lett.* **2008**, *100*, No. 123004.
(13) Niklasson, A. M. N.; Steneteg, P.; Bock, N. *J. Chem. Phys.* **2011**, *135*, No. 164111.
(14) Ohwaki, T.; Otani, M.; Ikeshoji, T.; Ozaki, T. *J. Chem. Phys.* **2012**, *136*, No. 134101.
(15) Ohwaki, T.; Otani, M.; Ozaki, T. *J. Chem. Phys.* **2014**, *140*, No. 244105.
(16) Shimojo, F.; Hattori, S.; Kalia, R. K.; Kunaseth, M.; Mou, W.; Nakano, A.; Nomura, K.-i.; Ohmura, S.; Rajak, P.; Shimamura, K.; Vashishta, P. *J. Chem. Phys.* **2014**, *140*, No. 18A529.
(17) Tsuchida, E. *J. Phys.: Condens. Matter* **2008**, *20*, No. 294212.
(18) Cawkwell, M. J.; Niklasson, A. M. N. *J. Chem. Phys.* **2012**, *137*, No. 134105.
(19) Li, X.-P.; Nunes, R. W.; Vanderbilt, D. *Phys. Rev. B* **1993**, *47*, 10891−10894.
(20) Hernández, E.; Gillan, M. J. *Phys. Rev. B* **1995**, *51*, 10157−10160.
(21) Hernández, E.; Gillan, M. J.; Goringe, C. M. *Phys. Rev. B* **1996**, *53*, 7147−7157.
(22) Bowler, D. R.; Miyazaki, T.; Gillan, M. J. *J. Phys.: Condens. Matter* **2002**, *14*, 2781−2798.
(23) Bowler, D. R.; Choudhury, R.; Gillan, M. J.; Miyazaki, T. *Phys. Status Solidi B* **2006**, *243*, 989−1000.
(24) Hernández, E.; Gillan, M. J.; Goringe, C. M. *Phys. Rev. B* **1997**, *55*, 13485−13493.
(25) Torralba, A. S.; Todorović, M.; Brázdová, V.; Choudhury, R.; Miyazaki, T.; Gillan, M. J.; Bowler, D. R. *J. Phys.: Condens. Matter* **2008**, *20*, No. 294206.
(26) Bowler, D. R.; Gillan, M. J. *Comput. Phys. Commun.* **1999**, *120*, 95−108.
(27) McWeeny, R. *Rev. Mod. Phys.* **1960**, *32*, 335−369.
(28) Palser, A. H. R.; Manolopoulos, D. E. *Phys. Rev. B* **1998**, *58*, 12704−12711.
(29) As each support function is represented by only one PAO, we need not consider the time evolution of **S**.
(30) Press, W. H.; Flannery, B. P.; Teukolsky, S. A.; Vetterling, W. T. *Numerical Recipes in FORTRAN: The Art of Scientific Computing*, 2nd ed.; Cambridge University Press: Cambridge, U.K., 1992.
(31) Niklasson, A. M. N.; Steneteg, P.; Odell, A.; Bock, N.; Challacombe, M.; Tymczak, C. J.; Holmström, E.; Zheng, G.; Weber, V. *J. Chem. Phys.* **2009**, *130*, No. 214109.
(32) This does not affect the results, and larger basis sets are used below.
(33) Perdew, J. P.; Zunger, A. *Phys. Rev. B* **1981**, *23*, 5048−5079.
(34) Verlet, L. *Phys. Rev.* **1967**, *159*, 98−103.
(35) This does not mean that the result of MD using R_L = 13 bohr is incorrect. The different trajectory may simply come from infinitesimal differences in forces of a chaotic system.
(36) Souvatzis, P.; Niklasson, A. M. N. *J. Chem. Phys.* **2014**, *140*, No. 044117.
(37) Perdew, J. P.; Burke, K.; Ernzerhof, M. *Phys. Rev. Lett.* **1996**, *77*, 3865−3868.
(38) Torralba, A. S.; Bowler, D. R.; Miyazaki, T.; Gillan, M. J. *J. Chem. Theory Comput.* **2009**, *5*, 1499−1505.
(39) Miyazaki, T. Ultra-Large-Scale First-Principles Calculations by the K Computer. *NIMS NOW Int.* **2013** *11* (9), 6; http://www.nims.go.jp/eng/publicity/nimsnow/2013/vol11_09.html (accessed Sept 22, 2014).